Research Square

Preprints are preliminary reports that have not undergone peer review.
They should not be considered conclusive, used to inform clinical practice,
or referenced by the media as validated information.

Response Surface Modelling and Optimization of Pineapple Leaf Fiber Reinforced Epoxy Composites Using Fiber Length and Loading

Vishal Wankhade

mevishal220311@gmail.com

Amity University Jaipur

Rajeev Sharma

Amity University Jaipur

Manoj Sharma

Swami Vivekanand College of Engineering

Priyanka Potghan

Swami Vivekanand College of Engineering

Shashi Chandra Sharma

Acropolis Institute of Technology and Research

Research Article

Keywords: sustainable materials, natural fiber composites, quadratic response surface-based regression model, statistical adequacy, surface and interaction analysis

Posted Date: November 19th, 2026

DOI: https://doi.org/10.21203/rs.3.rs-11328007/v1

License: This work is licensed under a Creative Commons Attribution 4.0 International License.
Read Full License

Additional Declarations: No competing interests reported.

Response Surface Modelling and Optimization of Pineapple Leaf Fiber Reinforced Epoxy Composites Using Fiber Length and Loading

Vishal Wankhade[1], Rajeev Sharma[2], Manoj Sharma[3], Priyanka Potghan[4,] Shashi Chandra Sharma[5]

[1]Ph.D. Scholar, Mechanical Engineering Department, Amity University Rajasthan, Jaipur, India, 303007, Email - mevishal220311@gmail.com

[2]Assistant Professor, Chemical Engineering Department, Amity University Rajasthan, Jaipur, India, 303007

[3,4]Assistant Professor, Mechanical Engineering Department, Swami Vivekanand College of Engineering, Indore, India, 452020

[5]Professor, Mechanical Engineering Department, Acropolis Institute of Technology and Research, Indore, India,453771

Corresponding Author: **Vishal Wankhade**

Address: Amity University SP-1, Kant Kalwar, RIICO Industrial Area, NH-11C, Jaipur, Rajasthan, 303007

Contact Number: +91-8878844446

Email: mevishal220311@gmail.com

Abstract

The demand for sustainable materials has started to draw the attention of engineers and researchers toward natural fiber composites. Pineapple fruit crop is a ratoon crop, and pineapple leaves are generated as an agricultural residue during cultivation and harvesting. The fiber generated from this residue pineapple leaves become an alternative for the managing this crop waste and to generate ecofriendly product. The present study includes the composite specimen fabrication of total 40 experimental framework using different combination pineapple fiber length (FL) and fiber content (FC) as a reinforcing elements and epoxy polymer as a reinforcement constituent. Further these specimens are experimentally evaluated using the ASTM standards to find out mechanical response in terms of tensile strength (TS), flexural strength (FS) and impact strength (IS) properties. The mechanical response of PLAF reinforced polymer composite depends upon the material variables such as FL and FC. The present research proposes a quadratic response surface-based regression model which is fitted to 40 runs for 5 x 8 full factorial data sets, for predicting multi-response optimization of the material variables. This research also includes determination of the statistical adequacy of the proposed model and surface and interaction analysis of the

material variables. The quadratic response surface-based regression model predicted compromise region at a fiber length of 22.6 mm and fiber proportion of 31.3 wt% with predicted mechanical response of tensile, flexural and impact strength of 48.91 MPa, 72.72 MPa and 6.51 kJ/m² respectively. In comparision experimental analysis represents that composite sample PF 29 with FL of 20 and FC of 30 wt% exhibits highest values of TS, FS and IS of 56.75 MPa, 87.85 MPa and 7.84 kJ/m², respectively. The developed quadratic response surface-based regression model exhibited coefficients of determination (R^2) for TS, FS and IS of 0.8869, 0.8816 and 0.8571 respectively, with corresponding adjusted R^2 values of 0.8703, 0.8642 and 0.8360. The extremely low p-values ($p< 0.05$) of 3.997×10^{-15}, 8.549×10^{-15} and 2.048×10^{-13} for tensile, flexural and impact performance respectively show that quadratic regression models are statistically significant.

Keywords: sustainable materials, natural fiber composites, quadratic response surface-based regression model, statistical adequacy, surface and interaction analysis

Abbreviations

PALF - Pineapple Leaf Fiber
RSM - Response Surface Methodology
QRSR - Quadratic Response Surface Regression
SD - Standard Deviation
TS - Tensile Strength
FS - Flexural Strength
IS - Impact Strength
ANOVA - Analysis of Variance
NaOH - Sodium Hydroxide
ASTM - American Society for Testing and Materials
CIPET - Central Institute of Petrochemicals Engineering & Technology

1. Introduction

The demand for sustainable materials has started to draw the attention of engineers and researchers toward natural fiber composites. This material inculcates natural fibers as a load bearing, reinforcing agent for composites and offering environment friendly and green substituted for synthetic fiber composites [1]. Pineapple fruit crop is a ratoon crop, and pineapple leaves are generated as an agricultural residue during cultivation and harvesting. The fiber generated from this residue pineapple leaves become an alternative for managing this crop waste and to generate ecofriendly friendly product [2]. The fibers which are extracted from the pineapple plant leaves by decortication method and known as the pineapple fibers [3]. The pineapple fiber content cellulose in the range of 70-82 weight percentages (wt%), hemicellulose of 6-20 wt%, lignin of 5-12 wt% and density of 1.40–1.52 g/cm³ [4]. The pineapple fibers contain the abundant hydroxyl (–OH) groups on their surface, epoxy reign contain the reactive group which make strong interfacial bonds with hydroxyl functionalities. The good interfacial bonding among the matrix constituent and fiber facilitate to transmission of load from matrix to fiber [5]. Epoxy resin also shows good wetting of fibers which results in the reduction of voids and good surface finish. Epoxy resin has very low curing shrinkages tendency, which ensures the dimensional stability of the composite after the completion of curing [6,7]. Epoxy resin shows resistance to many chemicals and moisture. Epoxy resin also shows ease of processing with the pineapple fiber for preparing

composite with variable FL and FC [8]. The QRSR model can be applied when relationship establishment is required in between the independent material variables such as FL and FC and the response variable such as TS, FS and IS [9]. The QRSR model also helps to quantify the liner effect, curvature (quadratic effects), and interaction effects between the factors [10]. ANOVA can be applied over QRSR model for finding overall significance and statistical significance of the model [11].

The optimization of the FL and FC helps to identify the optimum value of reinforcement parameters for achieving the enhanced mechanical performance and facilitating the effective design and manufacturing of the composite.

The main objectives of present research are:

(i) To find optimize value of FL and FC for obtaining maximum TS, FS and IS.
(ii) To examine model adequacy, interaction and curvature effects.
(iii) To determine the multi-response compromise condition using desirability function approach

2. Literature Review

PALF is a promising reinforcement among the other natural fibers because it has high tensile strength, cellulose content and thermal stability, unlike the other lignocellulosic fibers [12]. Pineapple fibers demonstrate relatively reduced frictional resistance because of the formation of strong interfacial bond between the polymer matrix elements and reinforcement constituents which prevent the removal of material and delamination during sliding loading conditions [13]. The hand lay-up technique is one of the most efficient and cost-effective composite fabrication processes. It is employed when the small scale or experimental purpose composite fabrication is required. This process allows sufficient fiber- matrix interaction and can easily be manage variety of FL and FC. [14]. The 5% NaOH treated PLAF composite shows improved mechanical performance in comparison with to raw untreated PLAF composite. The NaOH treatment improves the flexural strength by 31% [15]. Permanganate ($KMnO_4$) treatment of pineapple fiber also improves the mechanical response of the developed composite by improving the reinforcement and matrix bonding properties [16]. The peroxide treatment also improves mechanical behaviour of PALF composites by modifying the fiber surface by generating the active sites on fiber surface resultant to improv interaction between fiber and matrix element [17].

3. Existing Limitations and Novel Contributions

Previous investigation of PLAF composite has mainly emphasized on evolution of the effect of FL, FC, fiber treatment and hybridization of fibers or individual mechanical properties. The limited attention given to concurrent analysis of effect of FL and FC on mechanical attribute. The present research strives to fulfil this gap by investigating simultaneously by experimental analysis and by developing a QRSR model for multi-response optimization and desirability analysis.

Most of the previous investigations has considered a limited number of reinforcement configurations of FL and FC. The present research considered 40 experimental trials consisting of five FL (5, 10, 15, 20 and 25 mm) and eight FC levels (5, 10, 15, 20, 25, 30, 35 and 40 wt%).

The present study combinedly analysed experimental characterization using ASTM standards and protocols with quadratic response surface regression, statistical adequacy assessment, interaction analysis and multi-response desirability optimization. It also provides comparison of experimental and model-predicted responses.

4. Materials and Experimental Method

4.1 Reinforcement and Matrix Material

The raw PALF purchased from Vruksha Composites, Tenali are first washed with normal tap water for removing the dust and surface impurity. After that these washed fibers are impressed in the 5% NaOH solution for 2 hours at room temperature by maintaining fiber to solution ratio of 1:20. After 2 hours the fibers are removed from the NaOH solution and thoroughly washed several times with normal tap water, followed by washing with distilled water. These washed fibers are dried at room temperature for 48 hours followed by drying in oven at 60-80 ^{0}C for 2-4 hours. This oven dried fiber later chopped in the desire lengths of 5,10,15,20 and 25mm. The Lapox Metalam System B manufactured by Atul India Limited are utilized as a matrix material for composite manufacturing. The polymer matrix resin is applied in the ratio of 2:1 (Resin: Hardener) as per the standard operating procedure given by the manufacturer.

4.2 Experimental Design

Two independent material variables such as FL and FC are taken in consideration. For FL five combinations of length such as 5, 10, 15, 20, and 25 mm are used and for FCtotal eight combination of varying contain such as 5, 10 15, 20, 25, 30, 35 and 40 wt% are used. Using this combination of FL and FC, total 40 experimental trial are taken in consideration. For each trial of experiment total three specimens are fabricated for TS, FS and IS testing, according to the ASTM standards. The mean values of TS, FS and IS are taken in the consideration.

4.3 Composite Fabrication

The randomly oriented PLAF Composite samples are fabricated with improved hand layup process by applying the various combination of FL and FC. In this process the reinforcement fibers are first mixed with the resin by agitation for four to five minutes and later on this mixture is poured in the mould. After pouring mixture of reinforcement elements and matrix elements the mould is covered by the metal plate and uniform pressure is applied through the specially designed C type clamps on the cover plate to ensure uniform surface finish and avoid void formation. This whole composite fabrication process is carried out at room temperature and whole mould is put up for 24 hours for curing. After completion of curing process, the specimens are removed from the mould. Total three specimens are manufactured for each experimental trail. The TS test samples are manufactured as per ASTM-D638-Type-I standard [18], FS test samples are manufactured as per ASTM-D790 standard [19] and IS test samples are manufactured as per ASTM-D6110 standard [20].

4.4 Mechanical Testings

The TS, FS and IS testing of the composites are performed at CIPET, Bhopal. For each test total three samples are tested and average value of each test is reported in Table1.

The TS test is carried out at the cross-head speed of a 2mm/min following the ASTM-D638-Type-I testing procedure, FS test carried out at same cross head speed by using ASTM-D790 testing procedure and Charpy IS test is conducted as per ASTM-D6110 testing procedure.

Table 1. Experimental design and mechanical attributes of PLAF reinforced epoxy composites with mean ± SD

Exp. No.	FL (mm)	FC (wt%)	TS (MPa) with SD	FS (MPa) with SD	IS (kJ/m²) with SD
PF1	5	5	16.25 ± 0.418	26.44 ± 0.957	2.02 ± 0.148
PF2	10	5	16.85 ± 0.492	26.95 ± 0.948	2.15 ± 0.142
PF3	15	5	17.05 ± 0.524	27.45 ± 0.992	2.43 ± 0.152
PF4	20	5	17.68 ± 0.587	28.25 ± 1.121	2.88 ± 0.164
PF5	25	5	17.15 ± 0.612	27.13 ± 1.245	2.05 ± 0.143
PF6	5	10	20.22 ± 0.515	32.88 ± 1.257	2.57 ± 0.167
PF7	10	10	21.18 ± 0.567	34.13 ± 1.358	2.91 ± 0.179
PF8	15	10	23.17 ± 0.589	36.52 ± 1.112	3.05 ± 0.168
PF9	20	10	23.94 ± 0.592	38.12 ± 1.324	3.15 ± 0.192
PF10	25	10	22.54 ± 0.624	35.89 ± 1.425	2.98 ± 0.198
PF11	5	15	27.12 ± 0.652	41.45 ± 1.438	3.57 ± 0.246
PF12	10	15	28.34 ± 0.718	44.26 ± 1.527	3.97 ± 0.257
PF13	15	15	30.15 ± 0.724	47.35 ± 1.624	4.15 ± 0.278
PF14	20	15	32.25 ± 0.717	49.49 ± 1.758	4.45 ± 0.295
PF15	25	15	31.34 ± 0.754	47.13 ± 1.425	4.05 ± 0.298
PF16	5	20	34.27 ± 0.864	52.58 ± 1.789	4.65 ± 0.294
PF17	10	20	36.75 ± 0.926	56.74 ± 1.825	4.98 ± 0.315
PF18	15	20	38.82 ± 0.985	58.38 ± 1.868	5.11 ± 0.346
PF19	20	20	40.27 ± 1.005	64.28 ± 1.958	5.45 ± 0.334
PF20	25	20	39.28 ± 0.945	59.26 ± 1.987	5.05 ± 0.356
PF21	5	25	40.25 ± 1.01	65.49 ± 1.969	5.08 ± 0.378
PF22	10	25	41.75 ± 1.067	66.11 ± 1.979	5.25 ± 0.365
PF23	15	25	44.86 ± 1.215	70.16 ± 2.125	5.45 ± 0.359
PF24	20	25	48.78 ± 1.325	74.18 ± 2.238	5.89 ± 0.369
PF25	25	25	50.64 ± 1.551	70.19 ± 2.268	6.12 ± 0.376
PF26	5	30	46.14 ± 1.357	74.14 ± 2.268	6.29 ± 0.394
PF27	10	30	49.74 ± 1.346	75.66 ± 2.298	6.95 ± 0.447
PF28	15	30	52.28 ± 1.419	82.35 ± 2.325	7.12 ± 0.496
PF29	20	30	56.75 ± 1.421	87.85 ± 2.548	7.84 ± 0.498
PF30	25	30	55.15 ± 1.595	79.95 ± 2.527	7.58 ± 0.487
PF31	5	35	42.27 ± 1.268	70.25 ± 2.425	6.04 ± 0.374
PF32	10	35	46.98 ± 1.698	72.68 ± 2.398	6.86 ± 0.487

PF33	15	35	49.24 ± 1.652	73.87 ± 2.368	7.02 ± 0.492
PF34	20	35	52.45 ± 1.842	74.74 ± 2.425	7.27 ± 0.458
PF35	25	35	51.25 ± 1.762	73.19 ± 2.328	7.12 ± 0.449
PF36	5	40	32.17 ± 1.115	50.45 ± 2.258	4.75 ± 0.498
PF37	10	40	35.79 ± 1.325	54.25 ± 2.369	4.85 ± 0.525
PF38	15	40	37.55 ± 1.327	56.83 ± 2.768	5.12 ± 0.415
PF39	20	40	39.25 ± 1.456	60.27 ± 2.825	5.35 ± 0.468
PF40	25	40	36.74 ± 1.528	57.46 ± 2.815	5.05 ± 0.523

The Figs. 1–3 illustrate SD error bars for the experimental results tabulated in Table 1 for TS, FS and IS respectively.

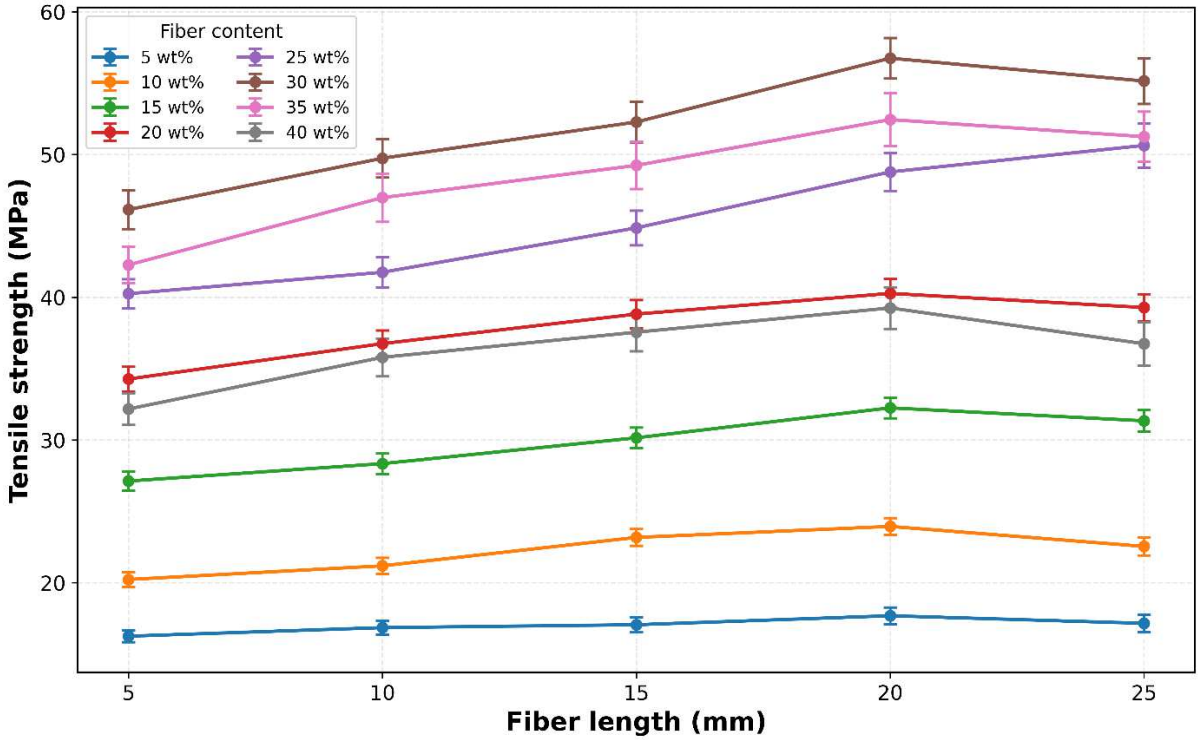


Fig. 1. Experimental TS of PLAF composite with SD error bars.

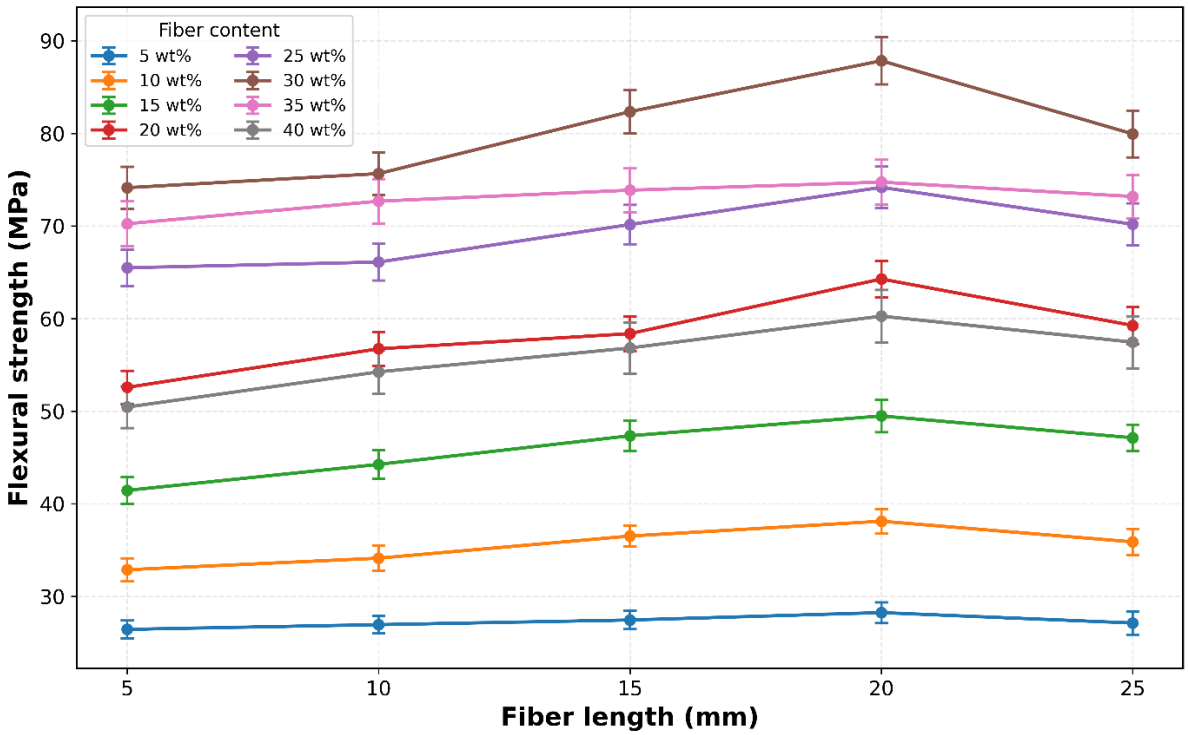


Fig. 2. Experimental FS of PLAF composite with SD error bars.

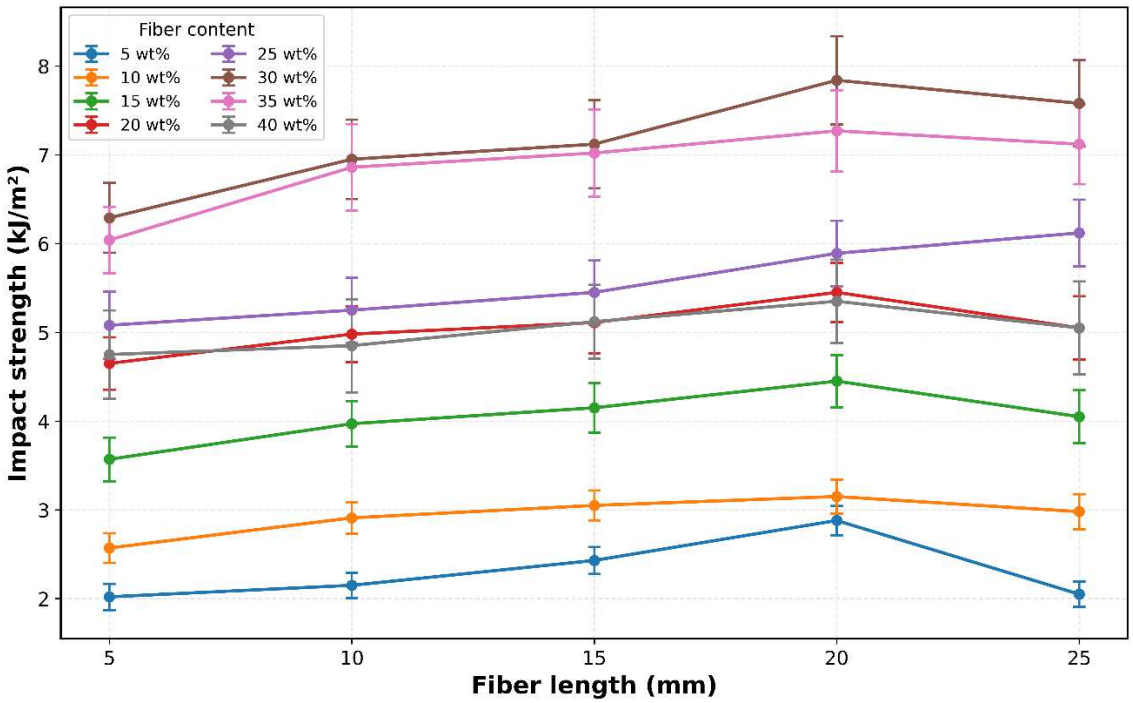


Fig. 3. Experimental IS of PLAF composite with SD error bars.

4.5 Main-Effect Analysis of FL and FC

The main effect analysis represents the average influence of FL and FC on the TS, FS and IS of PLAF composite. Table 2 shows the main-effect analysis of FL on mechanical properties and Table 3 shows the main-effect analysis of FC on the mechanical response.

Table 2. Main-effect means of FL on mechanical response.

FL (mm)	Mean TS (MPa)	Mean FS (MPa)	Mean IS (kJ/m²)
5	32.336	51.71	4.371
10	34.672	53.848	4.74
15	36.64	56.614	4.931
20	38.921	59.648	5.285
25	38.011	56.275	5

The main-effect analysis of FL shows that the peak values of mechanical response obtained at the FL of 20mm.

Table 3. Main-effect means of FC on mechanical response.

PALF Content (wt%)	Mean TS (MPa)	Mean FS (MPa)	Mean IS (kJ/m²)
5	16.996	27.244	2.306
10	22.21	35.508	2.932
15	29.84	45.936	4.038
20	37.878	58.248	5.048
25	45.256	69.226	5.558
30	52.012	79.99	7.156
35	48.438	72.946	6.862
40	36.3	55.852	5.024

The main-effect analysis of FC shows that the peak values of mechanical response obtained at the FC of 30 wt%.

4.6 Quadratic response surface-based regression (QRSR) modelling and multi-response optimization

The QRSR model was fitted to the 40 experimental trails obtained from a 5 × 8 full-factorial arrangement, considering five different FL (5, 10, 15, 20 and 25 mm) and eight different FC (5–40 wt%, at 5 wt% intervals). Thus, the model development is performed using the experimental full-factorial dataset rather than a conventional central composite design (CCD) or Box–Behnken design (BBD).

4.6.1 Definition of experimental factors and responses

Table 4 represents independent variables, their symbol, actual range and coded value respectively.

Table 4 Symbol, actual range and coded value of independent variables.

Factor	Symbol	Actual range	Coded variable
Fiber length	L	5–25 mm	x_1
Fiber content	C	5–40 wt%	x_2

4.6.2 Coding of experimental variables

The experimental variables are converted into dimensionless coded variables for QRSR modelling

The general coding formulation applied are as:

$$x_i = \frac{X_i - X_0}{\Delta X_i} \qquad (1)$$

where:

X_i= actual value of factor
X_0= selected center value
ΔX_i= coding interval
x_i= coded value
L = FL at maximum TS, FS and IS
C = FC at maximum TS, FS and IS

For FL:

$$X_0 = \frac{5 + 25}{2} = 15mm$$

and

$$\Delta X_0 = \frac{25 + 5}{2} = 10$$

Therefore,

$$x_1 = \frac{L - 15}{10}$$

For FC:

$$X_0 = \frac{5 + 40}{2} = 22.5\ wt\%$$

and

$$\Delta X_2 = \frac{40 - 5}{2} = 17.5$$

Therefore,

$$x_2 = \frac{C - 22.5}{17.5}$$

As the experimental levels are not symmetrical and not distributed around a common centre because of it code zero is chosen for mathematically preferable values.

Fiber length

5 → −1
10 → −0.5
15 → 0

20 → +0.5
25 → +1

Fiber loading

5 → −1
10 → −0.7143
15 → −0.4286
20 → −0.1429
25 → +0.1429
30 → +0.4286
35 → +0.7143
40 → +1

4.6.3 Coded experimental design matrix

Using the coding transformation, the experiments are coded and tabulated in the Table 5

Table 5. Coded Experimental Design Matrix for the QRSR

Exp. No.	x_1	x_2	x_1x_2	x_1^2	x_2^2
PF1	-1	-1	1	1	1
PF2	-0.5	-1	0.5	0.25	1
PF3	0	-1	0	0	1
PF4	0.5	-1	-0.5	0.25	1
PF5	1	-1	-1	1	1
PF6	-1	-0.7143	0.71429	1	0.51020
PF7	-0.5	-0.7143	0.35714	0.25	0.51020
PF8	0	-0.7143	0	0	0.51020
PF9	0.5	-0.7143	-0.3571	0.25	0.51020
PF10	1	-0.7143	-0.7143	1	0.51020
PF11	-1	-0.4286	0.42857	1	0.18367
PF12	-0.5	-0.4286	0.21429	0.25	0.18367
PF13	0	-0.4286	0	0	0.18367
PF14	0.5	-0.4286	-0.2143	0.25	0.18367
PF15	1	-0.4286	-0.4286	1	0.18367
PF16	-1	-0.1429	0.14286	1	0.02041
PF17	-0.5	-0.1429	0.07143	0.25	0.02041
PF18	0	-0.1429	0	0	0.02041
PF19	0.5	-0.1429	-0.0714	0.25	0.02041
PF20	1	-0.1429	-0.1429	1	0.02041
PF21	-1	0.14286	-0.1429	1	0.02041
PF22	-0.5	0.14286	-0.0714	0.25	0.02041
PF23	0	0.14286	0	0	0.02041
PF24	0.5	0.14286	0.07143	0.25	0.02041
PF25	1	0.14286	0.14286	1	0.02041

PF26	-1	0.42857	-0.4286	1	0.18367
PF27	-0.5	0.42857	-0.2143	0.25	0.18367
PF28	0	0.42857	0	0	0.18367
PF29	0.5	0.42857	0.21429	0.25	0.18367
PF30	1	0.42857	0.42857	1	0.18367
PF31	-1	0.71429	-0.7143	1	0.51020
PF32	-0.5	0.71429	-0.3571	0.25	0.51020
PF33	0	0.71429	0	0	0.51020
PF34	0.5	0.71429	0.35714	0.25	0.51020
PF35	1	0.71429	0.71429	1	0.51020
PF36	-1	1	-1	1	1
PF37	-0.5	1	-0.5	0.25	1
PF38	0	1	0	0	1
PF39	0.5	1	0.5	0.25	1
PF40	1	1	1	1	1

4.6.4 Second-order response surface model

For two independent material variables (FL and FC), the QRSR equation can be written as:

$$Y = \beta_0 + \beta_1 x_1 + \beta_2 x_2 + \beta_{12} x_1 x_2 + \beta_{11} x_1^2 + \beta_{22} x_2^2 + \varepsilon \qquad (2)$$

where:

Y= predicted response
β_0= intercept
β_1, β_2= linear coefficients
β_{12}= interaction coefficient
β_{11}, β_{22}= quadratic coefficients
x_1= coded fiber length
x_2= coded fiber loading
ε= random error

Three separate models of QRSR equation are developed because there are three responses (TS, FS and IS).

4.6.5 Matrix formulation of QRSR

The regression equation can be represented in the matrix form as:

$$Y = X\beta + \varepsilon \qquad (3)$$

For every experimental run:

$$X = [1 \quad x_1 \quad x_2 \quad x_1 x_2 \quad x_1^2 \quad x_2^2]$$

Therefore, the design matrix for 40 experiments:

$$X_{40\times 6} = \begin{bmatrix} 1 & x_{11} & x_{21} & x_{11}x_{21} & x_{11}^2 & x_{21}^2 \\ 1 & x_{12} & x_{22} & x_{12}x_{22} & x_{12}^2 & x_{22}^2 \\ \vdots & \vdots & \vdots & \vdots & \vdots & \vdots \\ 1 & x_{1,40} & x_{2,40} & x_{1,40}x_{2,40} & x_{1,40}^2 & x_{2,40}^2 \end{bmatrix}$$

The response vector is:

$$Y = \begin{bmatrix} Y_1 \\ Y_2 \\ \vdots \\ Y_{40} \end{bmatrix}$$

and the coefficient vector is:

$$\beta = \begin{bmatrix} \beta_0 \\ \beta_1 \\ \beta_2 \\ \beta_{12} \\ \beta_{11} \\ \beta_{22} \end{bmatrix}$$

The least-squares estimator is:

$$\hat{\beta} = (X^T X)^{-1} X^T Y \qquad (4)$$

The same design matrix is used for all three responses (TS, FS and IS) because the 40 factor combinations are identical.

Table 6 is representing intercept, linear coefficients, interaction coefficient and quadratic coefficients for three responses (TS, FS and IS).

Table 6. Estimated Coefficients and Model Adequacy Parameters of the QRSR Model

Response	β_0	β_1	β_2	β_{12}	β_{11}	β_{22}	R^2	Adj. R^2	RMSE
TS	43.796	3.11975	14.1734	1.68542	-1.7654	-15.86	0.8869	0.8703	4.0292
FS	67.3118	2.986	20.8578	1.07833	-3.0721	-23.7	0.8816	0.8642	6.0372
IS	5.8262	0.3605	2.0225	0.14383	-0.3271	-1.86	0.8571	0.836	0.6228

ensile-strength RSM model

$$Y_T = 43.7960 + 3.1198x_1 + 14.1734x_2 + 1.6854x_1x_2 - 1.7654x_1^2 - 15.8598x_2^2 \quad (5)$$

Flexural strength RSM model

$$Y_F = 67.3118 + 2.9860x_1 + 20.8578x_2 + 1.0783x_1x_2 - 3.0721x_1^2 - 23.6995x_2^2 (6)$$

Impact strength RSM model

$$Y_I = 5.8262 + 0.3605x_1 + 2.0225x_2 + 0.1438x_1x_2 - 0.3271x_1^2 - 1.8600x_2^2 (7)$$

The positive linear coefficients in the tensile, flexural and impact equation represents that the particular performance increases with the increasing FL and FC initially up to a certain limit. The negative quadratic coefficient in the equation represents curvature and reduction in TS, FS and IS beyond the optimum condition of FL and FC.

For FL and FC the optimization algorithm lies within:

$$5 \leq L \leq 25 \text{ mm}$$

and

$$5 \leq C \leq 40 \text{ wt\%}.$$

At the optimum,

$$L = 22.6 \text{ mm}$$

and

$$C = 31.3 \text{ wt\%}.$$

Therefore,

$$x_1 = \frac{22.6 - 15}{10} = \frac{7.6}{10} = 0.7600$$

and

$$x_2 = \frac{31.3 - 22.5}{17.5} = \frac{8.8}{17.5} = 0.50286$$

Substitute the value of x_1 and x_2 in QRSR equations (eq. no. 5,6 and 7)

$$Y_T = 43.7960 + 3.1198(0.7600) + 14.1734(0.502857) + 1.6854(0.7600)(0.502857) - 1.7654(0.7600)^2 - 15.8598(0.502857)^2$$

$$Y_T \approx 48.91 \text{ MPa}$$

$$Y_F = 67.3118 + 2.9860(0.7600) + 20.8578(0.502857) + 1.0783(0.7600)(0.502857) - 3.0721(0.7600)^2 - 23.6995(0.502857)^2$$

$$Y_F \approx 72.72 \text{ MPa}$$

$$Y_I = 5.8262 + 0.3605(0.7600) + 2.0225(0.502857) + 0.1438(0.7600)(0.502857) - 0.3271(0.7600)^2 - 1.8600(0.502857)^2$$

$$Y_I \approx 6.51\ kJ/m^2$$

QRSR model predicted TS, FS and IS as 48.91 MPa, 72.72 MPa and 6.51 kJ/m^2 respectively at FL of 22.6 mm and FC of 31.30 wt%.

Table 7 shows the predicted value of TS, FS and IS for different combination of FL and FC.

Table 7. Predicted value of mechanical response

Exp. No.	FL (mm)	FC (wt%)	TS (MPa)	FS (MPa)	IS (kJ/m²)
PF1	5	5	10.563	17.775	1.400
PF2	10	5	12.604	21.033	1.754
PF3	15	5	13.763	22.754	1.944
PF4	20	5	14.039	22.940	1.970
PF5	25	5	13.432	21.590	1.833
PF6	5	10	21.899	35.034	2.848
PF7	10	10	24.181	38.446	3.222
PF8	15	10	25.580	40.322	3.433
PF9	20	10	26.097	40.662	3.480
PF10	25	10	25.731	39.465	3.363
PF11	5	15	30.646	48.424	3.992
PF12	10	15	33.169	51.990	4.387
PF13	15	15	34.809	54.020	4.618
PF14	20	15	35.566	54.514	4.685
PF15	25	15	35.441	53.471	4.590
PF16	5	20	36.803	57.944	4.832
PF17	10	20	39.567	61.664	5.248
PF18	15	20	41.448	63.848	5.499
PF19	20	20	42.446	64.496	5.588
PF20	25	20	42.561	63.608	5.512
PF21	5	25	40.371	63.596	5.369
PF22	10	25	43.375	67.470	5.805
PF23	15	25	45.497	69.808	6.077
PF24	20	25	46.736	70.610	6.186
PF25	25	25	47.092	69.876	6.131
PF26	5	30	41.350	65.378	5.602
PF27	10	30	44.595	69.406	6.059
PF28	15	30	46.957	71.898	6.351
PF29	20	30	48.912	72.724	6.512
PF30	25	30	49.034	72.274	6.446
PF31	5	35	39.739	63.290	5.532
PF32	10	35	43.225	67.472	6.008
PF33	15	35	45.828	70.119	6.322
PF34	20	35	47.549	71.229	6.472
PF35	25	35	48.386	70.803	6.458
PF36	5	40	35.539	57.334	5.157
PF37	10	40	39.266	61.670	5.655
PF38	15	40	42.110	64.470	5.989
PF39	20	40	44.071	65.734	6.159

PF40	25	40	45.149	65.462	6.166

4.6.6 Statistical Adequacy of the QRSR Model

The coefficient of determination is calculated as:

$$R^2 = 1 - \frac{SS_E}{SS_T} \quad (8)$$

where:

$$SS_E = \sum_{i=1}^{n} (Y_i - \hat{Y}_i)^2 \quad (9)$$

and

$$SS_T = \sum_{i=1}^{n} (Y_i - \bar{Y})^2 \quad (10)$$

Table 8 shows coefficient of determination (R^2) , adjusted R^2, F-statistic values, RMSE values and p-values for developed response surface formulation

Table 8 Statistical Adequacy of the Developed QRSR Model

Response	R^2	Adjusted R^2	RMSE	Overall F	p-value
Tensile strength	0.8869	0.8703	4.0292	53.33	3.997×10^{-15}
Flexural strength	0.8816	0.8642	6.0372	50.64	8.549×10^{-15}
Impact strength	0.8571	0.8360	0.6228	40.77	2.048×10^{-13}

4.6.7 Comparison of Experimental and Model-Predicted Responses

The comparison of experimental results with the predicted results are presented by the parity plot analysis as represented in figure 4 - 6. The experimental values are plotted against the QRSR models predicted values, while the agreement between both values are denoted by diagonal line. The parity plots provide a direct graphical representation of how closely the fitted equations reproduce the experimental behaviour over the investigated range.

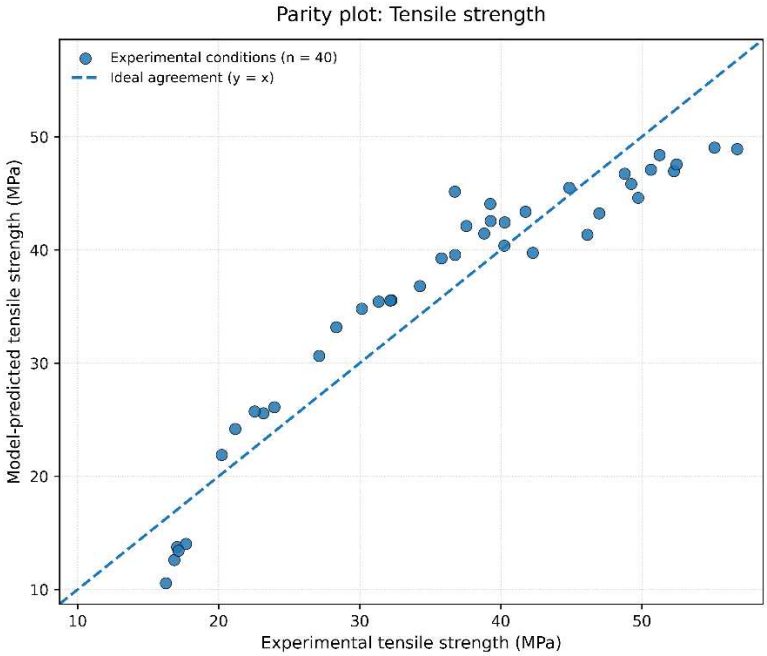


Fig. 4. Parity plots comparison of experimental and QRSR models prediction of TS.

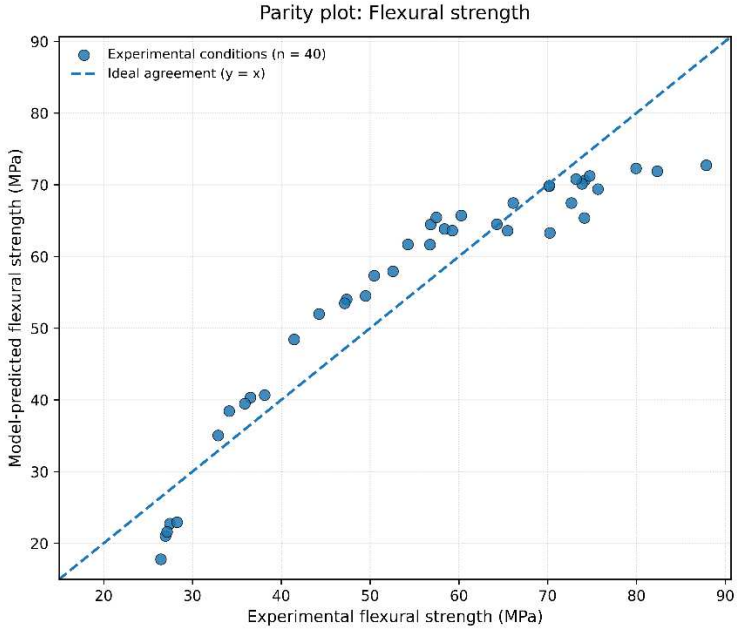


Fig. 5. Parity plots comparison of experimental and QRSR models prediction of FS.

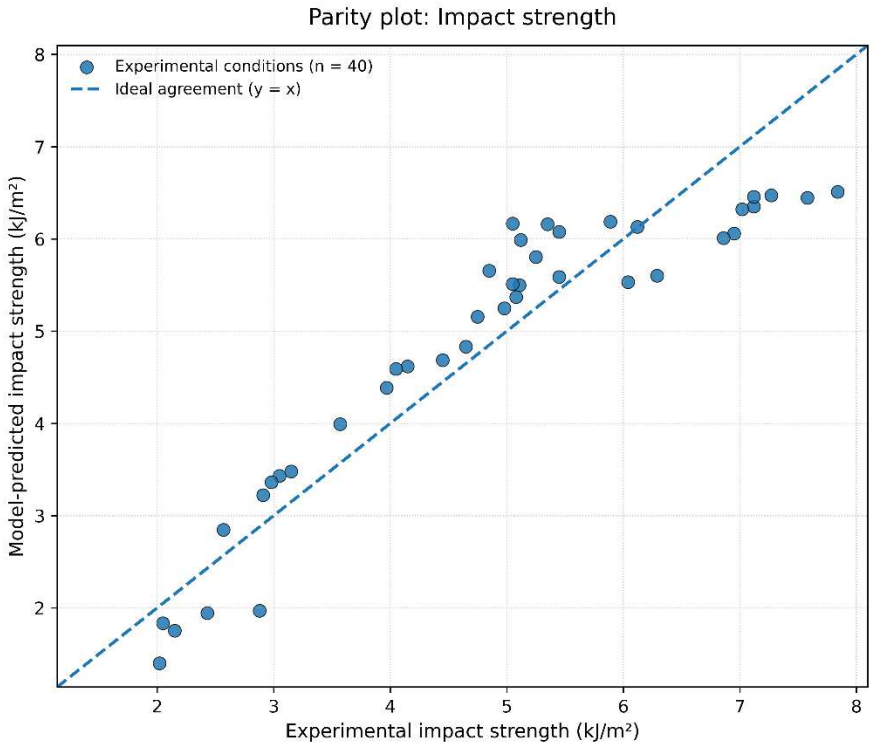


Fig. 6. Parity plots comparison of experimental and QRSR models prediction of IS.

4.6.8 Response Surface and Interaction Analysis

The combined effect of the reinforcement FL and FC on mechanical performance is graphically represented by the response surface. Unlike a single factor at a time graphical representation, the response surface represents continuous graphical demonstration of the fitted response within the investigated factor domain. The figure 7 shows quadratic response surface for TS, the figure 8 represent quadratic response surface for FS and figure 9 shows quadratic response surface for IS.

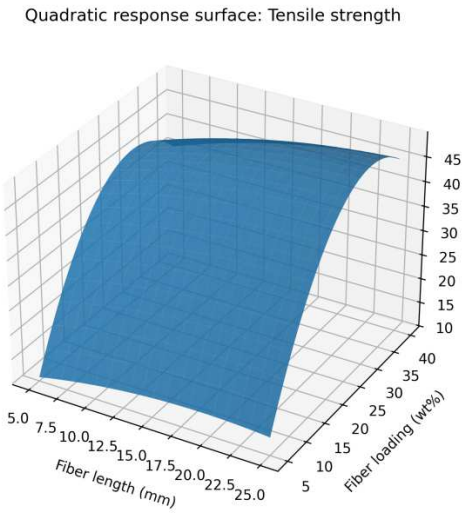


Fig. 7. Quadratic response surface for TS.

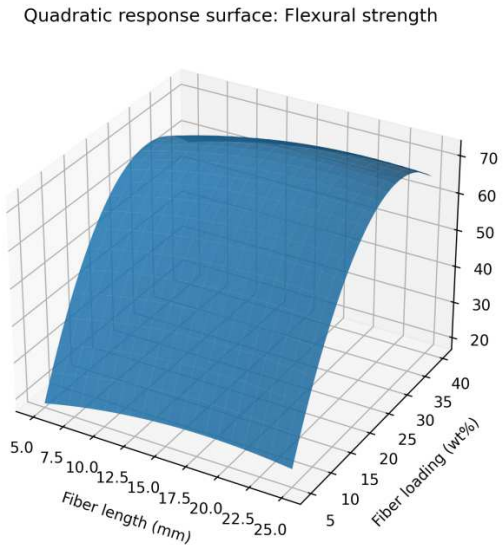


Fig. 8. Quadratic response surface for FS.

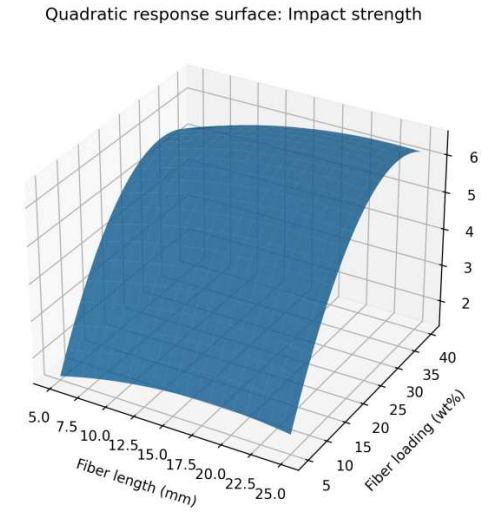


Fig. 9. Quadratic response surface for IS.

Figures 7 to 9 graphically represent three response surfaces, which exhibit a distinctly curved profile rather than a simple linear or planar trend. The positive interaction terms obtained for the quadratic models of TS, FS and IS demonstrate that the effect of one factor influences and varies according to the level of the other factor. The fitted surfaces show rise up to an optimum value of FL and FC beyond that optimum limit curvature in the response domain with negative quadratic coefficients are observed. These may represent that above optimum level tensile, flexural and impact performance declines.

4.6.9 Multi - response optimization

Multi-response optimization represents the best suitable optimum combination of FL and FC which favour to achieve the peak mechanical performance. Three mechanical responses TS, FS and IS are assigned equal weightage and treated for larger-the-better responses because the objective was to identify a balanced mechanical-performance condition. The equal weighting was also adopted by considering a neutral multi-response decision rule because no application-specific priority among these three responses was considered. The normalized desirability, for response i, was formulated as:

$$d_i = \begin{cases} 0, & Y_i < Y_{i,min} \\ \left(\frac{Y_i - Y_{i,min}}{Y_{i,max} - Y_{i,min}}\right)^s, & Y_{i,min} \le Y_i \le Y_{i,max} \\ 1, & Y_i > Y_{i,max} \end{cases} \quad (11)$$

Where,
Y_i - predicted response,
$Y_{i,min}$ - lower limits of the response,
$Y_{i,max}$- upper limits of the response,
d_T - desirability values for TS
d_B - desirability values for FS
d_I - desirability values for IS
The experimental response ranges used for desirability calculation were

$$16.25 \le T \le 56.75\ MPa$$
$$26.44 \le F \le 87.85\ MPa$$
$$2.02 \le I \le 7.84\ kJ/m^2$$

Therefore, the individual desirability functions for the three mechanical responses were expressed as
for TS,

$$d_T = \frac{T - 16.25}{56.75 - 16.25}$$

or

$$d_T = \frac{T - 16.25}{40.50}$$

for FS,

$$d_F = \frac{F - 26.44}{87.85 - 26.44}$$

or

$$d_F = \frac{F - 26.44}{61.41}$$

for IS,

$$d_I = \frac{I - 2.02}{7.84 - 2.02}$$

or

$$d_I = \frac{I - 2.02}{5.82}$$

$$D = (d_T d_F d_I)^{1/3}$$

The multi-response optimization of the developed QRSR models resulted in an optimum FL of

$$L^* = 22.6\ mm$$

and optimum FC of

$$C^* = 31.3\ wt\%$$

At this optimized condition, the quadratic models predicted

$$T^* = 48.91\ MPa$$
$$F^* = 72.72\ MPa$$
$$I^* = 6.51\ kJ/m^2$$

for TS, FS and IS respectively.
The individual desirability for TS was calculated as

$$d_T = \frac{48.91 - 16.25}{56.75 - 16.25}$$
$$d_T = 0.8064$$

Similarly, the individual desirability for FS was

$$d_F = \frac{72.72 - 26.44}{87.85 - 26.44}$$
$$d_F = 0.7536$$

The individual desirability for IS was calculated *as*

$$d_I = \frac{6.51 - 2.02}{7.84 - 2.02}$$
$$d_I = 0.7715$$

For equal importance the overall desirability "D" is defined as:

$$D = (d_T d_F d_I)^{1/3} \qquad (12)$$

$$D = (0.8064 \times 0.7536 \times 0.7715)^{1/3}$$
$$D = 0.7769 \approx 0.777$$

The PF29 experimental trial which represents that composite sample consist FL of 20 mm and FC of 30 wt% exhibits TS of 56.75 MPa, FS of 87.85 MPa and IS 7.84 kJ/m². The QRSR model predicted optimum FL of 22.6 mm and optimum FC of 31.3 wt% at this optimum condition the predicted mechanical response is 48.91 MPa tensile strength, 72.72 MPa flexural strength, and 6.51 kJ/m² impact strength.

The RSM identified a model-predicted compromise region at a FL of 22.6 mm and a FC of 31.3 wt%, with predicted TS, FS and IS of 48.91 MPa, 72.72 MPa, and 6.51 kJ/m², respectively. These predicted values of mechanical attributes are obtained from the fitted QRSR and have not been validate by experimentally. The predicted optimization results of mechanical performance show lower values as compared to the corresponding experimental results of PF 29. This difference between the model prediction and experimental results shows requirement of the further refinement.

Figure 10 represents overall desirability map. It illustrates the effect of FL and FC on the TS, FS and IS and identifies the region which provides the most favourable simultaneous performance.

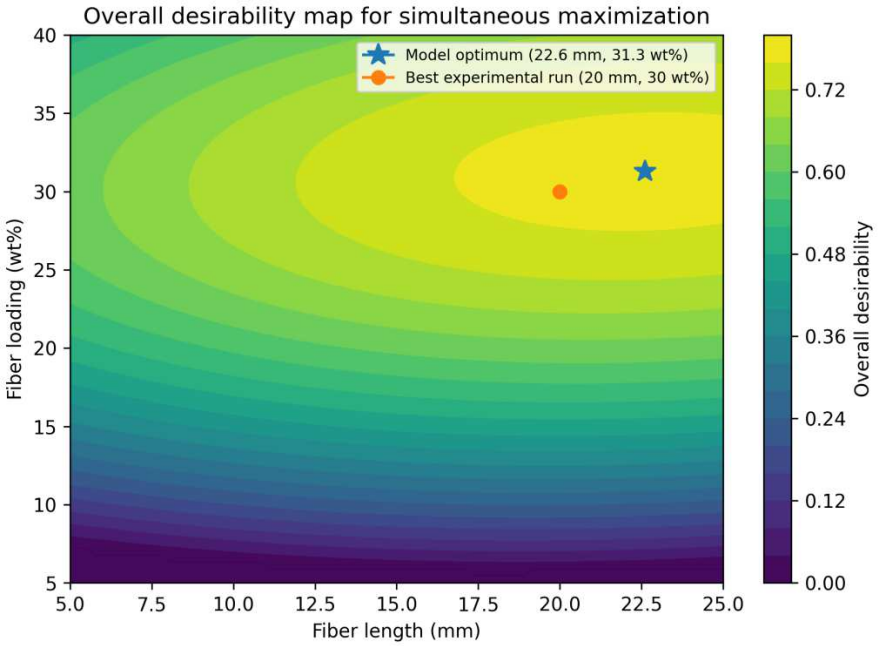


Fig. 10. Overall desirability map for model-predicted compromise region for FL and FC.

Figure 10 graphically represents that experimental results and model predicted values are located at optimum region in the overall desirability map and the model predicted performance results lie close to the PF29 experimental condition, particularly within the same intermediate-to-high FL and FC region.

5. Comparison with Published PALF/Epoxy Studies

Praveena Bindiganavile Anand et al. reported that the 5% NaOH treated, 20 – 25 mm long pineapple fiber with 15 wt% FC shows highest TS of 78 MPa and FS of 112 MPa [5].

Harishbabu, S et al. reported that PLAF reinforced epoxy composite exhibits highest TS and FS at 30 wt% FC as compared with other composite samples of 0,5,10 and 20 wt% of FC [21].

Hossain MA et al. investigated that PLAF epoxy composite with 30 wt% of FC shows highest TS of 51.6 MPa and impact toughness of approximately 14.189 kg/cm as compared with other composites fabricated with 10,15,20,25 wt% of FC [22].

6.Results and discussion.

6.1 Experimental Results

PALF composite specimen PF1 shows least value of TS, FS and IS as 16.25 MPa, 26.44 MPa and 2.02 kJ/m² respectively at FL of 5 mm and FC of 5 wt%. beyond this condition the mechanical performance shows rising trend with the raising contribution of FC and FL up to 20 mm. The PF 29 specimen shows maximum value of TS, FS and IS of 56.75MPa, 87.85 MPa and 7.84 kJ/m² respectively at FL of 20 mm and FC of 30 wt%. Beyond this limit the excess quantity of the reinforcement shows decline in the mechanical performance. The PF 30 sample shows TS, FS and IS of 55.15MPa, 79.95 MPa and 7.58 kJ/m² respectively at FL of 25mm and FC of 30 wt%. This decline in the mechanical performance may be resultant of

matrix starvation, void formation, localized fiber agglomeration and poor interaction bonding between fiber and matrix due to higher quantity of the reinforcement fibers.

6.2 RMS Modeling Optimization

The developed QRSR model identified a model-predicted condition at FL of 22.6 mm and FC of 31.3 wt%. Under this predicted condition, the predicted TS, FS and IS will be 48.91MPa, 72.72 MPa and 6.51 kJ/m², respectively. These predictions show relative difference of reduction of 13.81% for TS, 17.22% for the FS and 16.96 % for IS compared with the superior performance obtained by the experimental method. At the FL of 20mm and FC of 30 wt% the predicted TS, FS and IS model predictions at PF29's factor settings are predicted as 48.44 MPa, 72.85 MPa and 6.48 kJ/m², respectively. Further no independent confirmation experiment was conducted at the model-predicted condition and predicted response values are not considered experimentally verified.

6.3 Statistical Model Adequacy

For the developed RSM Coefficient of determination (R^2) of the fitted QRSR models are calculated as 0.8869, 0.8816, and 0.8571 for TS, FS and IS respectively. Which indicate that FL, FC and their interaction in the fitted models account for the 88.69%, 88.16%, and 85.71% of the observed response variance in the respective datasets. Relatively high Adjusted R^2values of 0.8703, 0.8642, and 0.8360 for TS, FS and IS respectively indicate the explanatory performance of the fitted models after accounting for the number of model terms.

The overall F-statistic values of 53.33, 50.64, and 40.77 for TS, FS and IS respectively indicate a strong overall regression effect.

The RMSE values of 4.0292 MPa, 6.0372 MPa and 0.6228 kJ/m² for TS, FS and IS respectively indicates lower deviation between the experimental observations and model-predicted responses.

The extremely low p-values of 3.997×10^{-15}, 8.549×10^{-15} and 2.048×10^{-13} for TS, FS and IS respectively show that QRSR models are statistically significant. The overall F-statistics values and its corresponding p-values shows that the fitted QRSR models are statistically significant at the 5% significance level.

6.4 Response Surface and Interaction Analysis

The combined influence of FL and FCon TS, FS and IS are graphically represented by response surfaces curves. The fitted surfaces show rise up to an optimum value of FL and FCbeyond that optimum limit curvature in the response domain with negative quadratic coefficients are observed. These may represent that above optimum level the mechanical response declines.

6.5 Desirability Analysis

The desirability map shows that the predicted results through Second-order response surface modelling and multi-response optimization lies approximately close around to the experimentally results for PF29 formulation which supports the developed model and research formulation can used as process-window tool.

The desirability approach provides a model-predicted compromise condition within the investigated FL and FC domain. As the predicted responses at the compromise region differs with the experimental measured responses of PF29, therefore desirability result should be interpreted as a preliminary model-based recommendation rather than a validated experimental optimum.

7. Conclusion

The present research investigated the influence of FL and FC on TS, FS and IS of PLAF reinforced epoxy polymer composite using 40 experimental frameworks. Based on the experimental results and statistical findings the following conclusions were drawn.

- The experimental analysis represents that composite sample PF 29 with FL of 20 and FC of 30 wt% exhibits highest values experimentally measured of TS, FS and IS of 56.75 MPa, 87.85 MPa and 7.84 kJ/m², respectively.
- The developed QRSR model identified a model-predicted compromise region at a FL of 22.6 mm and a FC of 31.3 wt%. For this compromise region the corresponding values of TS, FS and IS are predicted as 48.91 MPa, 72.72 MPa, and 6.51 kJ/m², respectively. All these values are representing model predictions and should not be interpreted as experimentally confirmed results.
- The developed QRSR model successfully expressed the relationships between material variables FL and FC and the three mechanical responses TS, FS and IS.
- Coefficient of determination for the developed regression model confirms that the FL and FC and their interaction cause variation in the TS, FS and IS.
- Relatively high Adjusted R^2valuesrepresent that the fitted terms contribute meaningfully to model performance The Overall F-statistic values indicate a strong overall regression effect. The extremely low p-values ($p < 0.05$) represents that quadratic regression models are statistically significant.
- The predicted negative quadratic coefficients associated with FL and FC represents the nonlinear relation between mechanical performance and processing parameters. At excessive reinforcement levels above the optimum condition the mechanical performance declines.

Data Availability

The datasets generated and analyzed during the current study are available from the corresponding author upon reasonable request.

Funding Declaration

The authors received no financial support for the research, authorship, or publication of this article.

Ethics, Consent to Participate, and Consent to Publish

Ethics, Consent to Participate, and Consent to Publish declarations: not applicable.

Clinical Trial Registration

The study does not involve a clinical trial. The applicable declaration is: “Clinical trial number: not applicable.”

References

1. Shifa, S. S., & Zhang, N. (2026). Progress and perspectives on plant-based natural fiber-reinforced polymer composites: Structure–property relationships and emerging design strategies. *Journal of Polymer Research, 33*, 254. https://doi.org/10.1007/s10965-026-04954-y

2. Zainol, N., Aziz, N. H., & Gopalan, T. E. (2026). Valorization of pineapple leaf waste as potential dielectric composite material using an optimized soda pulping process. *Discover Chemistry, 3*, 10. https://doi.org/10.1007/s44371-026-00471-5

3. Padzil, F. N. M., Ainun, Z. M. A., Abu Kassim, N., Lee, S. H., Lee, C. H., & Ariffin, H. (2020). Chemical, physical and biological treatments of pineapple leaf fibers. In M. Jawaid, M. Asim, P. Md. Tahir, & M. Nasir (Eds.), *Pineapple leaf fibers: Processing, properties and applications* (pp. 73–90). Springer, Singapore. https://doi.org/10.1007/978-981-15-1416-6_5

4. Sultan, M. T. H., et al. (2022). Dynamic and ballistic performance of uni- and bidirectional pineapple leaf fibers (PALF)-reinforced epoxy composites functionalized with graphene oxide. *Polymers, 14*(16), 3249. https://doi.org/10.3390/polym14163249

5. Bindiganavile Anand, P. (2026). Experimental evaluation of mechanical, tribological, and morphological characteristics of alkali-treated pineapple leaf fiber reinforced epoxy composites for structural and biomedical applications. *Journal of Engineering and Applied Science, 73*, 136. https://doi.org/10.1186/s44147-026-01000-y

6. Guedes, R. M., et al. (2025). En route to realistic sustainable structural fiber-reinforced polymers in a circular economy. *Advanced Composites and Hybrid Materials*. https://doi.org/10.1007/s42114-025-01508-6

7. Suresh, S., et al. (2017). A review on the mechanical modeling of composite manufacturing processes. *Archives of Computational Methods in Engineering*. https://doi.org/10.1007/s11831-016-9167-2

8. Rout, A. K., Satapathy, A., & Sahoo, S. (2016). Natural fiber-mediated epoxy composites – A review. *Composites Part B: Engineering, 99*, 425–435. https://doi.org/10.1016/j.compositesb.2016.06.051

9. Iliyasu, I., Bello, J. B., Dibal, M. N., Oyedeji, A. N., Salami, K. A., & Oyedeji, E. O. (2022). Response surface methodology for the optimization of the effect of fiber parameters on the physical and mechanical properties of deleb palm fiber reinforced epoxy composites. *Scientific African, 16*, e01269. https://doi.org/10.1016/j.sciaf.2022.e0126

10. Manjunatha, H. S., Kumar, S. S., Kumar, K. R., et al. (2026). Tribological optimization of bio-based microcrystalline cellulose and hybrid natural fiber reinforced epoxy composites using response surface methodology. *Scientific Reports, 16*, 24964. https://doi.org/10.1038/s41598-026-64852-7

11. Madhu, P., Sanjay, M.R., Senthamaraikannan, P., Pradeep, S., Sarojadevi, M., Khan, A. (2019). Optimization of tensile behavior of banana pseudo-stem (*Musa acuminate*) fiber reinforced epoxy composites using response surface methodology. *Journal of Materials Research and Technology, 8*(4), 3517–3528. https://doi.org/10.1016/j.jmrt.2019.06.026

12. Yadav, V. K., Verma, N., Kardam, S. K., & Pullela, M. (2025). Pineapple leaf fiber in polymer composites: Structure, characterization, and applications. *Materials Chemistry and Physics: Sustainability and Energy, 2*, 100011. https://doi.org/10.1016/j.macse.2025.100011

13. Louhichi, B., Joy, D., Sahu, S. K., Ayrilmis, N., Lee, I. E., Ngu, E. E., &Sundarasetty, H. (2026). Methods to optimize tribological properties of pineapple leaf fiber epoxy composites. *Industrial Crops and Products, 242*, 122865. https://doi.org/10.1016/j.indcrop.2026.122865

14. Hossain MA, Hossain MS, Khan RA, Chowdhury AMS (2022). Physico-mechanical properties enhancement of pineapple leaf fiber (PALF) reinforced epoxy resin-based composites using guar gum (polysaccharide) filler: effects of gamma radiation. *Radiation Effects and Defects in Solids*. 177(3–4):401–416. https://doi.org/10.1080/10420150.2022.2043317

15. Akarapoowadol, T., et al. Effect of alkali treatment on the mechanical and structural properties of pineapple leaf fiber for epoxy composite reinforcement. *ACS Omega* 11, 3974–3983 (2026). https://doi.org/10.1021/acsomega.5c07292

16. Hu, Y.W., Muchlis, A.M.G., Devi, R.K. *et al.* Biodegradable composite material by silane-modified pineapple leaf fiber with high flexibility and degradation rate. *ACS Sustainable Chemistry & Engineering* 13, 9728–9739 (2025). https://doi.org/10.1021/acssuschemeng.5c02699

17. Joseph, K., Pavithran, C. &Brahmakumar, M. Improved interactions in chemically modified pineapple leaf fiber reinforced polyethylene composites. *Composite Interfaces* 5, 3–12 (1998). https://doi.org/10.1163/156855498X00153

18. ASTM International. ASTM D638-22: Standard Test Method for Tensile Properties of Plastics. West Conshohocken, PA: ASTM International; 2022. https://doi.org/10.1520/D0638-22.

19. ASTM International. ASTM D790-25: Standard Test Methods for Flexural Properties of Unreinforced and Reinforced Plastics and Electrical Insulating Materials. West Conshohocken, PA: ASTM International; 2025. https://doi.org/10.1520/D0790-25.

20. ASTM International. ASTM D6110-26: Standard Test Method for Determining the Charpy Impact Resistance of Notched Specimens of Plastics. West Conshohocken, PA: ASTM International; 2026. https://doi.org/10.1520/D6110-26

21. Harishbabu, S., Elfar, A.A., Sreekanth, P.S.R., Sahu, S.K., Lee, I.E., Ngu, E.E. &Louhichi, B. Mechanical properties of pineapple leaf fiber reinforced epoxy composite. *BioResources***21**, 4792–4809 (2026). https://doi.org/10.15376/biores.21.2.4792-4809

22. Hossain MA, Hossain MS, Khan RA, Chowdhury AMS. Preparation and characterization of pineapple leaf fiber reinforced epoxy composite: effect of gamma radiation. *Adv Appl Sci* 7(3), 65–72 (2022). https://doi.org/10.11648/j.aas.20220703.15